

Development of a Scan Mirror Assembly
for an Extreme Ultraviolet Atmospheric Scanner

56-74
50434
125120 ✓

Thomas R. McBirney*

P 14

Abstract

A Scan Mirror Assembly (SMA) was created to rotate its SiC mirror through 8.5° in 90 seconds, then to return in 2 seconds, and repeating this motion continuously for at least three years.

Unique design features are:

- **Lightly preloaded, large angular-contact bearings.**
- Bearing preload using a **convoluted diaphragm.**
- Launch locks avoided by **static balancing.**
- Limited-scan rotation so **ball travel does not overlap.**
- **Silicon carbide mirror** on semi-kinematic mounts.

Introduction

Swales & Associates, Inc. was asked by the Naval Center for Space Technology to design and fabricate a Scan Mirror Assembly (SMA) for the Special Sensor/Ultraviolet Limb Imager (SSULI) Instrument for launch on the DMSP spacecraft. The SMA is expected to rotate its mirror through 8.5° in 90 seconds, then return in 2 seconds, repeating this motion continuously for at least three years with occasional excursion to 15° for cross calibration with other instruments. Figure 1 is a cross-section view of the SMA.

The SMA development program has resulted in the delivery of six flight articles. It also taught some lessons in spacecraft mechanism design, and these should be shared. Unique design features of the SMA are:

- **Lightly preloaded** (less than peak launch load), **angular-contact bearings** that are sized **larger** than the bearing loads would normally require.
- Bearing preload using a **convoluted diaphragm.**
- Launch locks avoided by **static balancing.**
- Limited scan rotation so **ball travel does not overlap.**
- A solid **silicon carbide mirror** on semi-kinematic mounts.

After design changes were made to eliminate failures of the diaphragm and mirror mounting, the SMA has successfully passed all system-level functional and environmental tests.

* Swales & Associates, Inc., Beltsville, MD

56059606 USI

Description

The SMA consists of an aluminum housing that supports several components:

- A 16-speed resolver stator.
- A DC torque motor stator.
- Two angular-contact ball bearings, which support a titanium shaft, which, in turn, supports the resolver and torque motor rotors and a mirror.

Description of Noted Features

Ball Bearings

The angular-contact Barden bearings are made with 440C races and TiC-coated 440C balls plated with "Demnum" grease. The retainer, made of Meldin 9000, is vacuum-impregnated with "Demnum" oil.

Lubrication

"Demnum" oil is a perfluoropolyether, low-outgassing lubricant made by Daiken Industries, Ltd. (Osaka, Japan). In recent NASA outgassing tests, its outgassing was measured at 0.00% CVCM (Collected Volatile Condensable Material) and 0.01% TML (Total Mass Loss), which is lower than any other known lubricant. (NASA Reference Publication 1124¹ lists Demnum L200 grease at 0.05% TML/0.00% CVCM and lists Demnum S200 oil at 0.12% TML/0.03% CVCM).

This lubricant was chosen as the best way to protect the delicate, far-ultraviolet reflecting surface of the mirror from molecular contamination.

There were considerable discussion and controversy regarding the use of this lubricant, since it is well-known that the perfluoropolyether lubricant family is known to suffer long-term chemical breakdown in the presence of iron/iron asperity contact that occurs in the boundary layer regime, and (since the scan speed is extremely slow) the bearings will operate continuously in that regime. This chemical breakdown is accelerated by the breakdown products themselves.

The proposed alternate lubricant was "Pennzane 2000" with 5% lead naphthanate added to provide boundary layer lubrication. Pennzane 2000 is listed in NASA Reference Publication 1124¹ as 0.42% TML/0.21% CVCM, and Pennzane 2000 with 5% Lead naphthanate is listed as 1.64% TML/0.19% CVCM, which raised concerns about mirror contamination. However, contemporary work at the Aerospace Corporation indicated that it was the solvent vehicle used to render lead naphthanate soluble in Pennzane 2000 (and not the lead naphthanate itself) that outgassed. This may well be correct, but no other solvent vehicle was proposed. In any event, the use of TiC-coated balls in our bearings eliminates the iron/iron asperity contact that causes Demnum to break down.

¹ Rev 2, dated November 1990, "Outgassing Data for Selecting Spacecraft Materials"

Preload

The bearing axial preload is set between 8 and 12 lbf to minimize rolling friction and power consumption during on-orbit operation. This very light preload is insufficient to withstand the inertial forces generated during launch vibration, so the bearing balls lose their preload at that time. To minimize impact loads, the maximum allowable axial travel is limited to between 0.008 and 0.012 in by a stainless steel spacer that bottoms out on a Titanium bearing bulkhead. Figure 2 depicts a typical force/deflection curve, and Figure 3 depicts the test setup used to measure it.

The bearing preload is provided by a convoluted diaphragm described below.

Convoluted Diaphragm

To control the very light axial bearing preload during operation, the outboard bearing is contained in a bearing carrier that is axially preloaded by the controlled deflection of a convoluted diaphragm.

The first design used a convoluted diaphragm formed from 304 CRES sheet that was electron beam welded to 304 CRES inner and outer machined rings. Unfortunately, I placed the welds in a high stress concentration area, so they cracked during vibration testing of the first SMA. This failure led to a re-design that used a CRES 17-7PH H900 convoluted diaphragm mechanically clamped at its inner and outer edges. I still feel a properly welded design that moved the welds to a lower stress area would save considerable weight, cost, and complexity.

The normal practice of using a slip fit at the outer bearing race to allow it to move axially in a fixed bulkhead was rejected due to the possibility of losing all control of the preload due to radial binding with thermal changes.

Flat diaphragms have also been used in spacecraft mechanisms to avoid thermal binding, but the limited OD/ID ratio available to the diaphragm in the SMA envelope would have severely limited their low spring rate travel range or would have required an unacceptably thin diaphragm. Adding a single shallow convolution to the diaphragm greatly increased the low spring rate travel range. The diaphragm is preloaded with a machined shim.

To measure the preload and the axial travel, the test setup shown in Figure 3 was used. A load cell, attached to a machine slide, imposed a bi-directional axial force on the SMA shaft, and an LVDT measured the resulting deflection. Both the load cell and LVDT outputs were recorded by a PC-based data acquisition system.

Figure 2 plots the deflection vs. force data recorded for a typical SMA. The spring rate of the diaphragm, the travel limits, and the bearing preload can be seen. The force level, which succeeds in starting motion by moving the shaft away from its preloaded position, is the bearing preload. Since the preload decreases as the spacer is made thinner, the initial preload is higher than the desired value, so the data of Figure 2 is taken several times as the spacer is gradually machined to its final thickness. This iterative process is accelerated by calculating the thickness to be removed based on the measured diaphragm stiffness and the desired change in preload. A suitable margin is inserted, since spacer thinning is obviously an irreversible act for a given spacer.

Optical/Electronic Alignment

To tag on-orbit scientific data from the SSULI Far Infrared Detector with the correct elevation angle, the angular relationship between the electrical resolver and the mirror must be accurately known. Although this correlation is finally performed on-orbit with known stars, the relationship must be set accurately enough during SMA assembly to preclude resolver rollover.

The electro-optical alignment jig shown in Figure 4 is used to locate the mirror in relation to the SMA housing, then null the resolver stator at the mid-position of the mirror travel. This jig is also used to set the spring-loaded travel stops.

To align the SMA housing with the alignment jig, a gauge block (used as a test mirror) is clamped to one side of the housing. A dowel pin is inserted into position 1 in the jig, then the SMA is centered in a pilot hole in the jig, and rotated until the test mirror autocollimates with a laser beam. The SMA is then clamped to the jig. The dowel pin is now removed, the jig rotated, and the pin placed in position 2.

Using an auxiliary clamp with twin adjustment screws (not shown in Figure 4), the SMA mirror is rotated until it is autocollimated with the laser beam. The resolver stator is rotated to electrically null the resolver output, then the stator is clamped.

Finally, the SMA and Jig are rotated to positions 3 and 4 in turn, and, at each position, the threaded, spring-loaded stops are adjusted to limit the maximum travel of the SMA shaft.

Static Balancing

Vibration, imposed along one axis during testing, will invariably couple into the other axes. In addition, flight vibration exists simultaneously along all three axes. Consequently, there is a possibility that, during vibration, the rotating parts of the SMA would rotate violently into the mechanical travel stops. To eliminate that possibility, many spacecraft scanners employ launch locks that are remotely released once on orbit.

To avoid the complexity of launch locks, the rotating parts of the SMA are statically balanced. The SMA also has four resolver rotor flex leads (redundant windings) and five mirror flex leads (three thermistor flex leads and 2 heater flex leads) that resist the rotational motion of the moving parts. Although it is desirable to minimize the angular

spring rate of these flex leads, they do perform a vital service during launch vibration. By forming the leads so that they exert zero torque near the center of mirror travel, they should tend to center the moving parts between the travel stops during vibration, thus preventing the SMA rotating parts from angular impact into those stops.

Limited Ball Travel

There was some concern that the very limited rotation of the scan motion would not allow the ball travel paths to overlap. This could lead to lubricant buildup in the races at the ends of the ball travel.

Silicon Carbide Mirror

The mirror is fabricated of solid silicon carbide for good reflectivity in the extreme ultraviolet and is mounted on three semi-kinematic supports to minimize mirror distortion due to differential thermal expansion between the SiC mirror and the titanium shaft. Figure 5 shows a schematic view of the three supports, which are designated flexures A, B, and C and simulate the kinematics of a ball in a socket, a ball in a groove, and a ball on a flat surface, respectively:

- Flexure A is a cruciform beam to allow 2 axis pivoting while restraining translations normal to and parallel to the mirror surface.
- Flexure B is a long small pin to allow 2 axis translation while restraining translation normal to the mirror surface.
- Flexure C is a long flat blade to allow single axis translation parallel to the mirror surface while restraining translation normal to the mirror surface.

The dimensions of the three flexural elements were selected by using an FEA model of the mirror, the flexures, and the shaft.

Test Results

Vibration Testing

As expected, the bearings did move freely during vibration testing. However, no damage to balls or races was experienced at any time.

There was one anomaly that was repeatedly observed, and is worth noting. Before and after each vibration test run, the SMA was functionally tested by scanning the mirror over its travel range, operating in a closed-position loop using its torque motor and resolver. The motor current was recorded versus scan position, thus providing a very sensitive indication of bearing friction and flex lead spring torque. Each pre-vibration functional test created a skewed rectangle with a motor current hysteresis of about 50 mA peak-to-peak (due to bearing friction of ± 0.005 N-m (± 0.35 in-lbf)) and a slope of 0.040 N-m/rad (5.7 in-lbf/rad) due to the flex lead spring rate.

However, every time we ran a post-vibration functional test, the motor current hysteresis increased to about 250 mA peak-to-peak *for only the first cycle of motion*. After a particular position had been passed once, the hysteresis loop up to that position returned to its pre-vibration level. Manually moving the mirror after the vibration table was turned off, *but before any other mirror motion had occurred*,

confirmed what the instrumentation told us — it was as if we had to push a barely noticeable “obstruction” out of the way. This phenomenon is currently unexplained but does not affect the SMA operation, since the torque motor has adequate margin to overcome it (maximum motor current can be 1,000 mA, which produces a torque of 1.6 N-m (14 in-lbf), and it disappears after the first scan motion.

Static Balancing

The static balancing, combined with the cable spring rate, successfully prevented stop contact during vibration testing. There was some initial concern that the flex leads would have to be carefully formed to bring the initial position to the center of travel, but this concern has diminished; contact during vibration has never been experienced.

Limited Ball Travel

Another phenomenon (not completely unexpected) was actually observed: When the scan angle was increased after many short scans had been performed, small “bumps” about 20 mA (= 0.002 N-m or 0.3 in-oz) high in the motor current were observed as the mirror moved past the end of travel of the short scans. These are currently attributed to a buildup of grease at the end of each ball track. However, after as few as 50 scan cycles that move past a bump, it gradually flattens out and disappears.

Silicon Carbide Mirror

The mirror was originally mounted on three semi-kinematic flexures that were attached to the mirror through three mounting holes in pockets at the edges of the mirror. However, after experiencing mirror pocket failures at flexure A during vibration, two parallel efforts were initiated to understand the problem:

1. several static load tests were performed that defined the static strength of the flexure A pocket, and
2. an analytical study was conducted to define the dynamic loads around that mirror pocket.

As a result of these efforts, two design changes were incorporated:

1. The flexure “A” mirror pocket was fitted with an Invar block retained by epoxy to spread the bending loads out as much as possible.
2. A “collar” was added to the original flexure “A” design, thus forming a second load bearing point against the shaft to reduce bending moments applied to the mirror by about a factor of 10 (Figure 6). Since this collar effectively provided the two-axis lateral restraint that was the function of the cruciform cross-section, that cross-section was changed to circular and reduced in size.

With these two changes, no further failures were experienced. In particular, the observed fracture pattern during a subsequent breakout test on a mirror pocket indicated excellent load coupling into the mirror.

It should be noted that the UTS of the SiC material was originally stated as 52 ksi, but later information indicated an actual average UTS of 20 ksi and a 3- σ low value of 9 ksi. In addition, subsurface defects were detected in one mirror by ultrasonic

scanning. However, as noted above, the Invar reinforcing block very effectively distributes the applied load into the mirror, so even this defect was acceptable. Table 1 is summary of the static load tests on the mirror pockets. Note that an intermediate design, using soft components to eliminate metal-to-SiC contact, also provided some improvement but was rendered unnecessary by the Invar block.

Table 1 - Mirror Static Load Test Summary

| Mirror # | Original design | Original design with flexure A-to-mirror interface cushioned with Vespel sleeve and soft aluminum washers | Flexure A with collar with Invar block |
|----------|--|--|--|
| #4-2 | | On 24 Feb 95, Pocket B broke at 75 lb On 1 Mar 95, Pocket C broke at 120 lb under pseudo-cyclic loading | |
| #2 | On 2 Feb 95, Pocket A broke at 45.18 lb, then Pocket C broke at 46.48 lb | | On 21 Apr 95, Pocket B broke at 194.40 lb |
| #1 | | | On 21 Apr 95, Pocket B did not break at 483.1 lb |

Lessons Learned

- Lightly preloaded, oversized ball bearings can survive space launch vehicle vibration levels to provide low-friction levels, thus minimizing on-orbit power consumption.
- Slightly anomalous ball bearing operation can be experienced immediately after vibration, but no long term effect is seen.
- Static balancing of rotating assemblies can be sufficient to eliminate launch locks.
- Structural attachments to silicon carbide mirrors must minimize and spread vibration-induced bending loads to avoid fracture.
- Convolute diaphragms, which provide a desirable combination of low axial and high radial spring rates, can be used successfully to provide precision support to scan mirror rotating shafts.

Acknowledgments

This work was sponsored by the Naval Research Laboratory, Washington, D.C. I want to thank Mr. Ed Devine of Swales for his invaluable guidance during this effort.

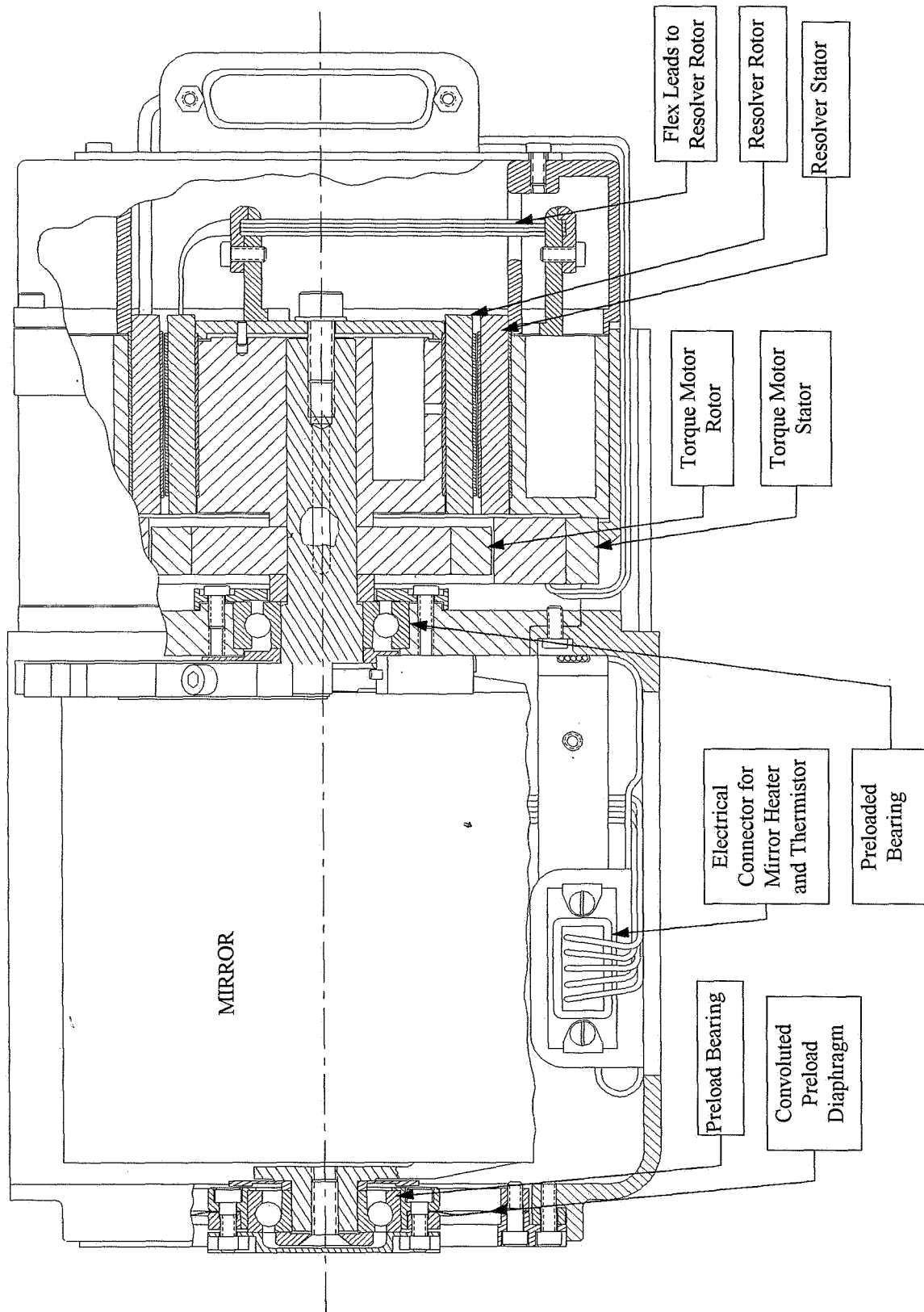


Figure 1 - Scan Mirror Assembly

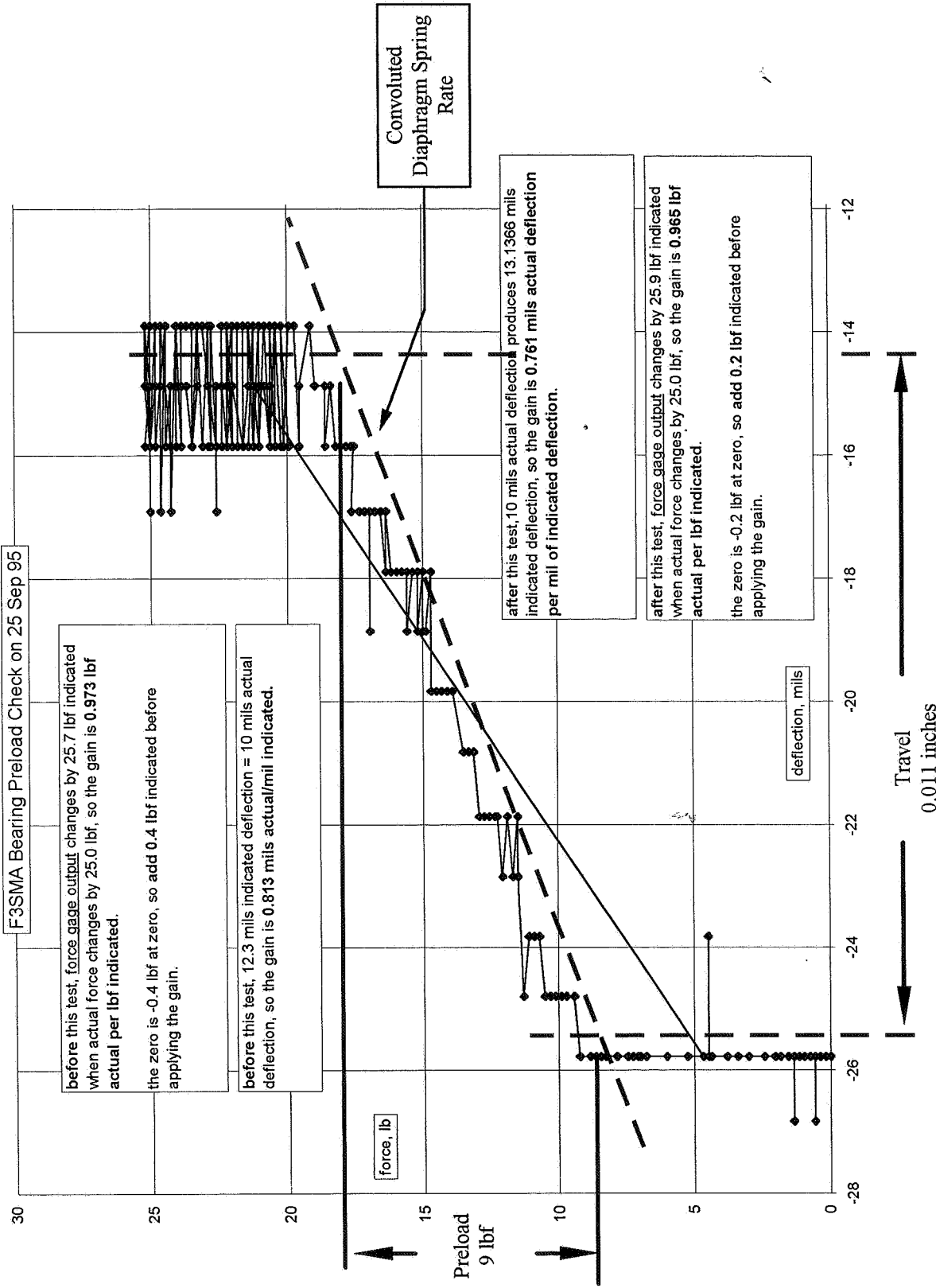


Figure 2 - Bearing Force/Deflection Curve

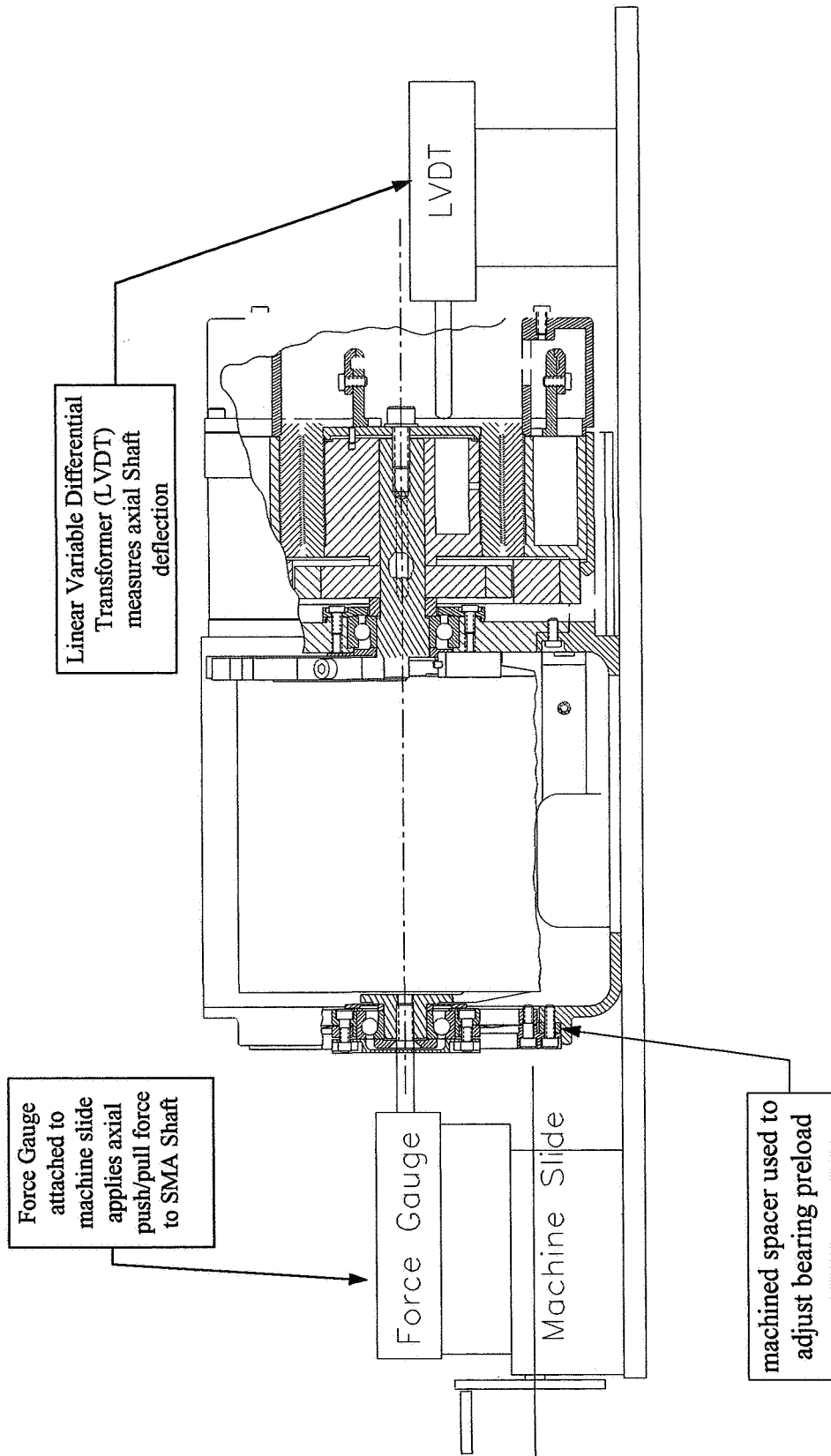


Figure 3 - SMA Bearing Test Setup

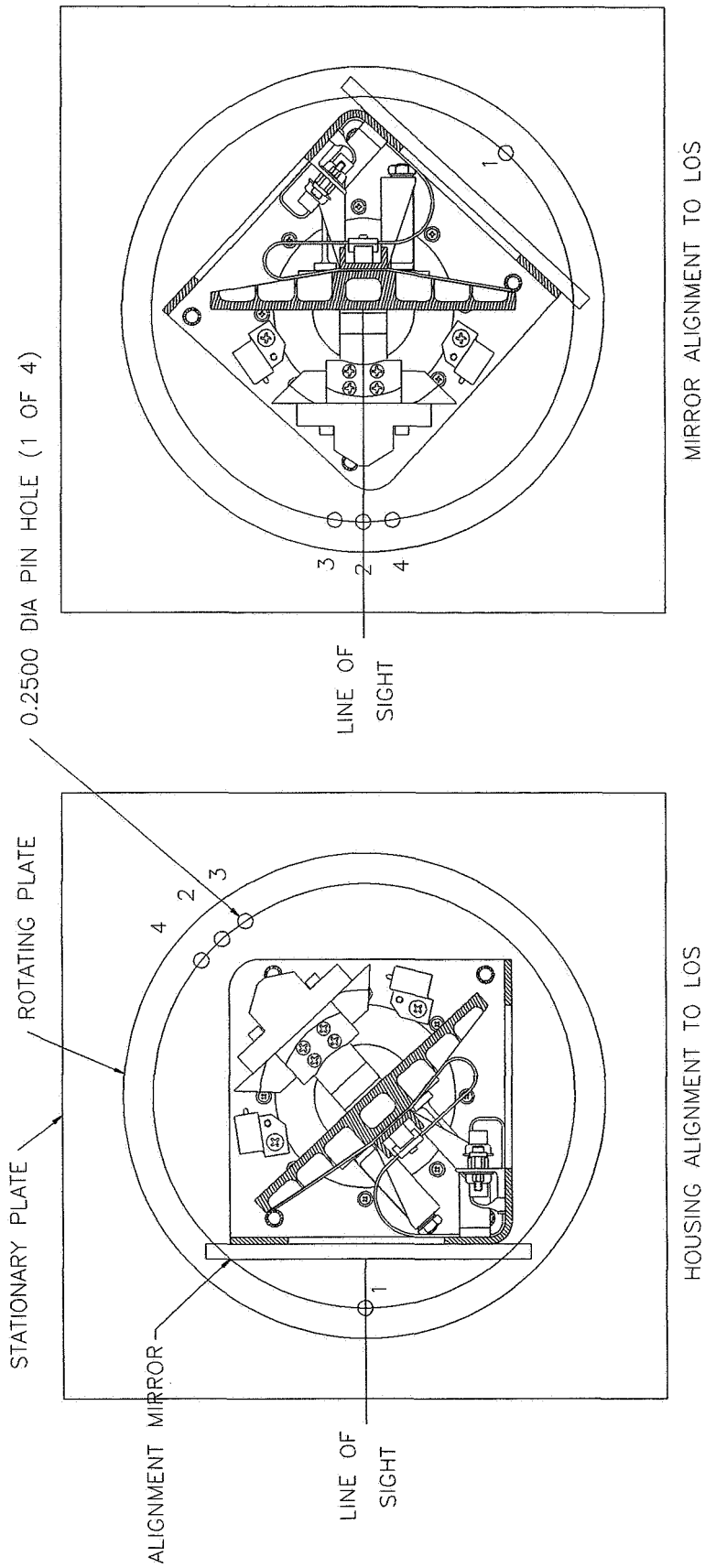


Figure 4 - Optoelec Alignment Jig

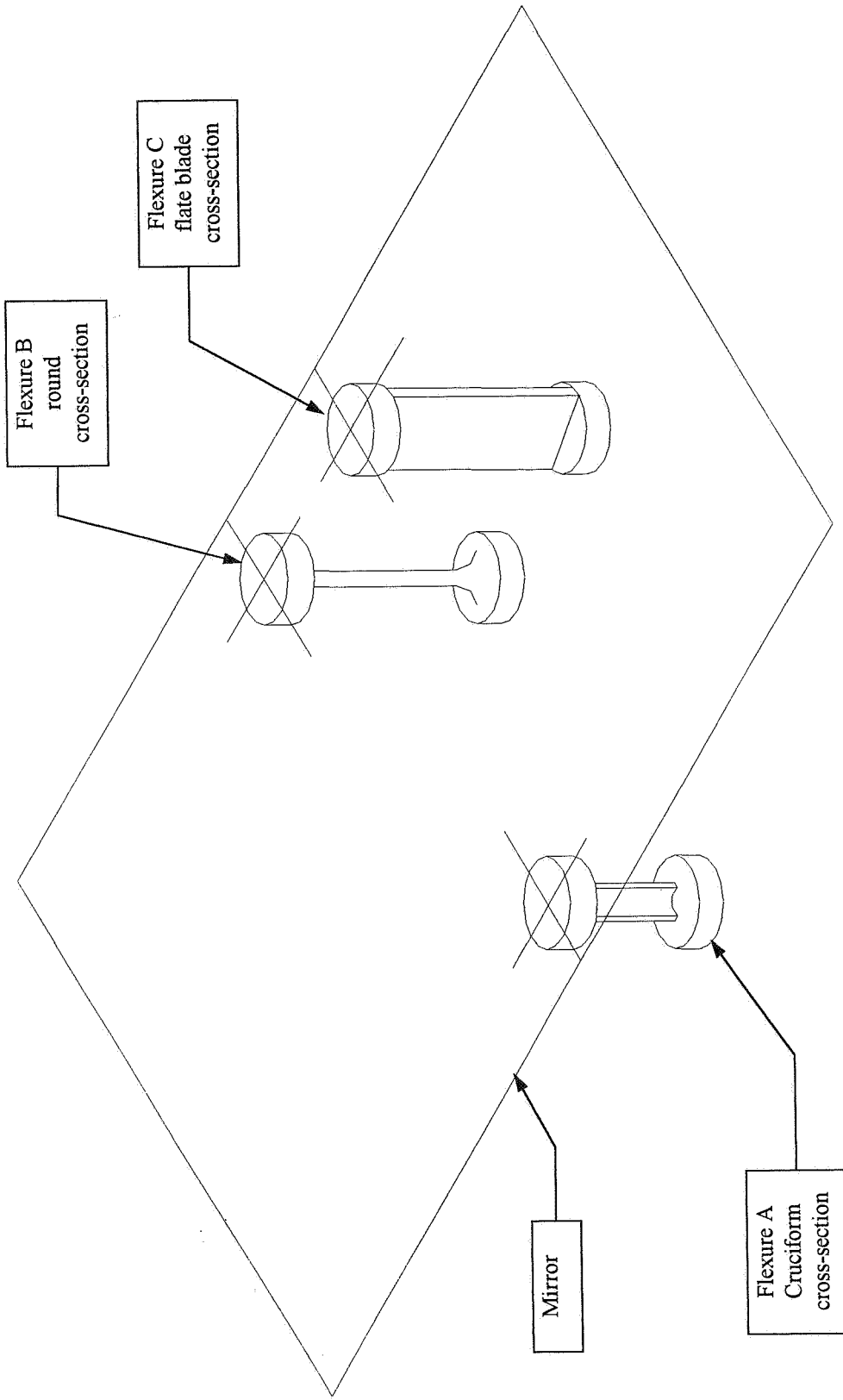


Figure 5 - Mirror Mount

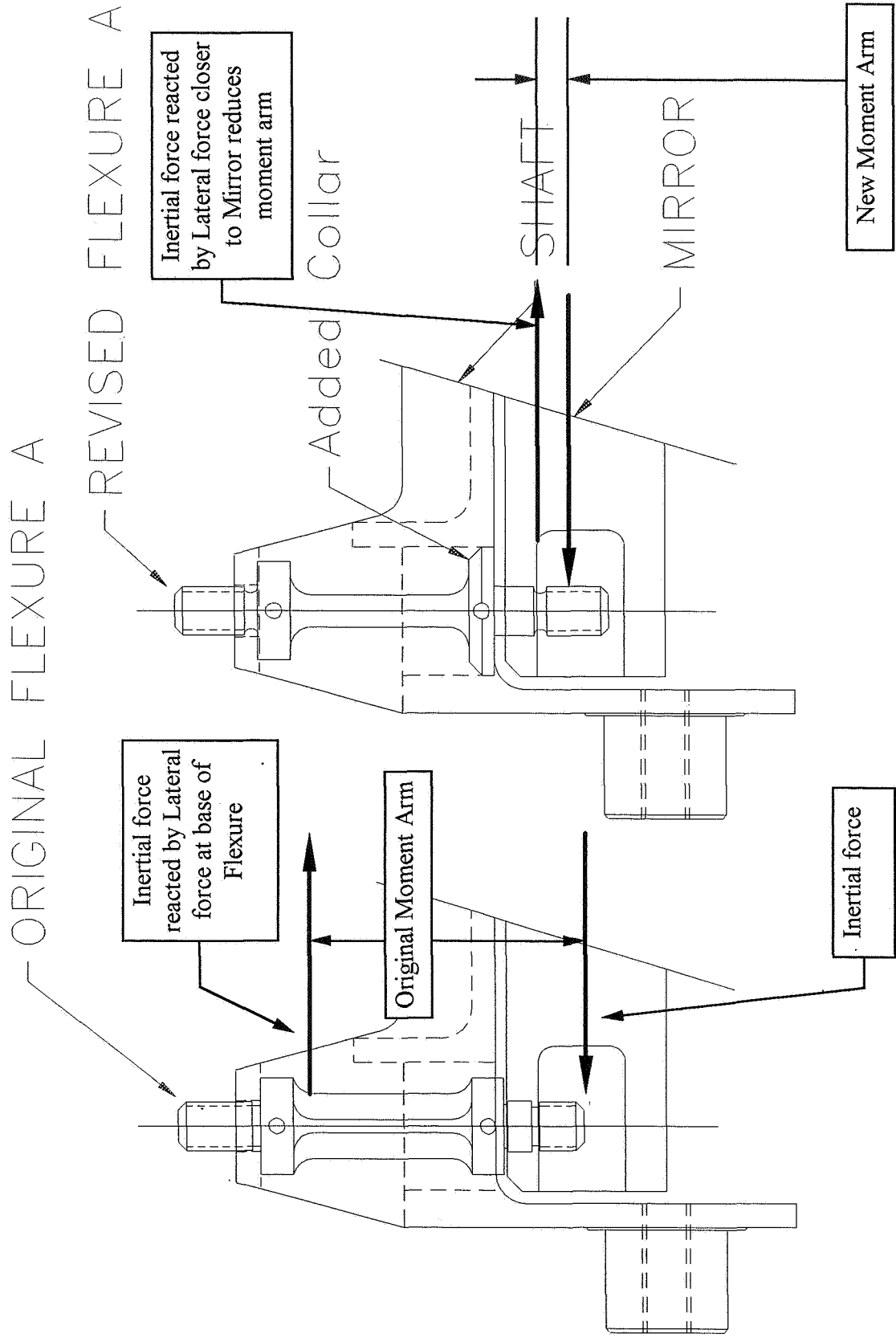


Figure 6 - Revised Flexure A